

Single-molecule diodes with high rectification ratios through environmental control

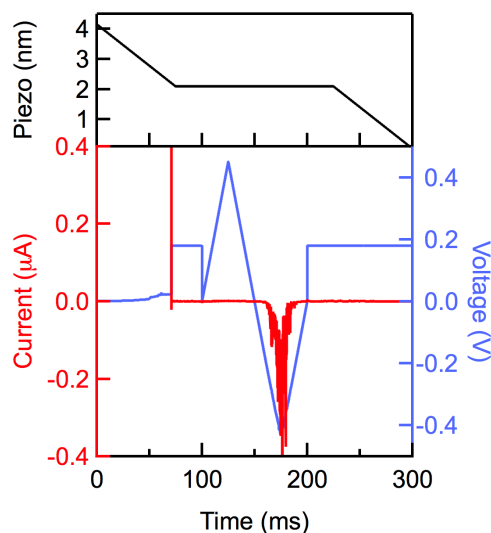
**Brian Capozzi, Jianlong Xia, Olgun Adak, Emma Dell, Zhen-Fei Liu, Jeffrey C. Taylor,
Jeffrey B. Neaton, Luis M. Campos and Latha Venkataraman**

Table of Contents

- I. Additional Data and Analysis
- II. Experimental Determination of Energy Level Alignment
- III. Computational Details
- IV. Synthetic Details & Characterization for TDO5
- V. References

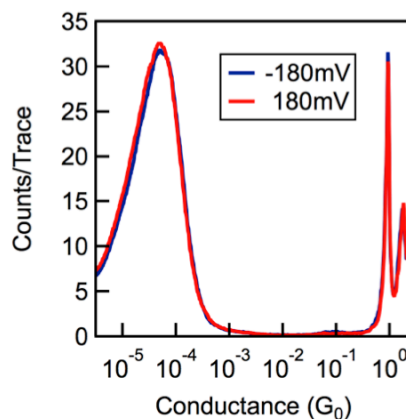
I. Additional Data & Analysis:

Sample IV Trace:



Supplementary Figure 1. Sample IV measurement. Top panel: Piezo ramp during a segment of the IV measurement. Bottom panel: Voltage applied to the tip (blue) and current flowing into the substrate (red) as a function of time for a single TDO4 trace in PC (same trace as in above panel). At -0.4V, a current of 0.4 μ A is measured, while at +0.4V, the current is very small.

TDO4 Histograms at +/-180mV in TCB:

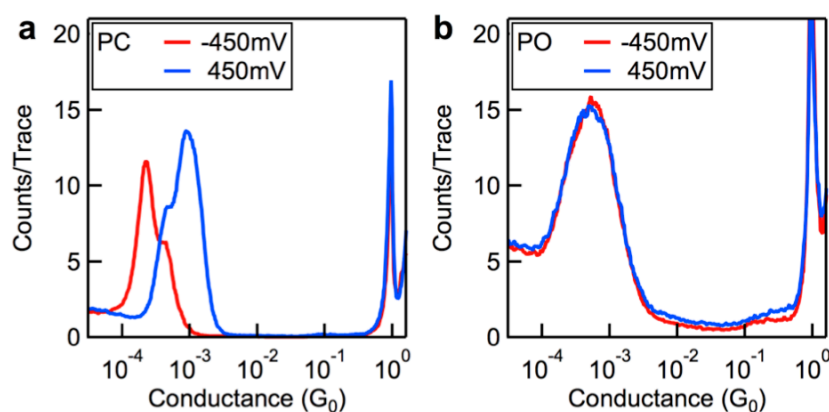


Supplementary Figure 2. Log-binned conductance histograms for TDO4 measured in 1,2,4-Trichlorobenzene at +/- 180mV using 100 bins/decade. In contrast with the data shown in Figure 1b, there is no change in conductance at the two different polarities.

Non-polar solvent with insulated tip

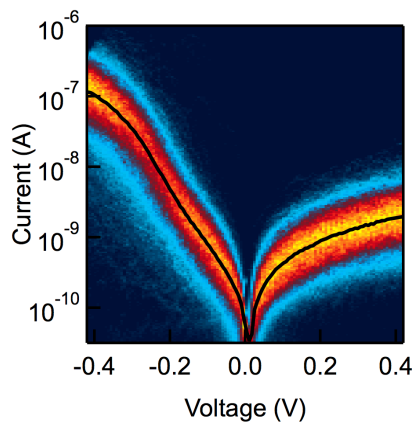
Measurements of 4,4''-Diamino-*p*-terphenyl were carried out in phenyl octane (PO, non-polar) and in propylene carbonate (PC, polar) with a coated tip (glue coated for PO, and wax

coated for PC). We collected 3000 conductance traces at +450mV and -450mV in both PC and PO (Figure S2). A clear shift in conductance is observed in PC while no change is seen in PO. We also note that 4,4''-Diamino-*p*-terphenyl has previously been shown to conduct through the highest occupied molecular orbital (HOMO)¹; its conductance shifts up at positive tip biases in PC.



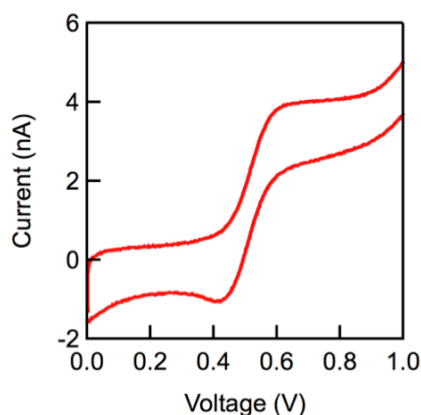
Supplementary Figure 3. Log-binned conductance histograms for 4,4''-diamino-*p*-terphenyl in (a) propylene carbonate (PC) and (b) phenyl octane (PO) created using 100 bins/decade. Both measurements were made with an insulated tip at 450mV and at -450mV. A clear polarity dependence is observed only in PC.

TDO4 IVs measured in propylene carbonate with an additional electrolyte



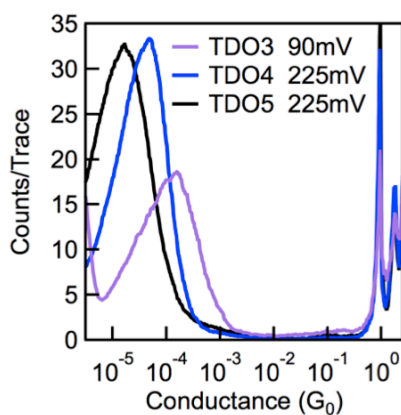
Supplementary Figure 4. Two-dimensional IV histogram for TDO4 measured in propylene carbonate with an additional 0.1M of tetrabutylammonium perchlorate. Histogram is constructed from 2671 traces.

Cyclic Voltammogram using Break-Junction geometry



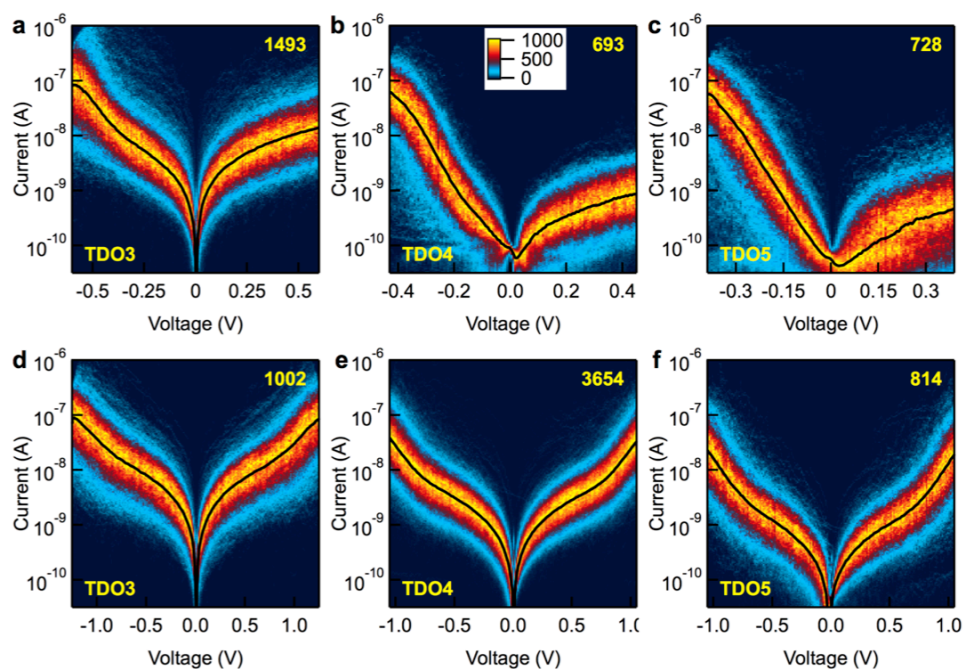
Supplementary Figure 5. Cyclic voltammogram taken using the break-junction geometry with a solution of 1mM ferrocene in propylene carbonate (there is no added supporting electrolyte). An insulated gold tip serves as our working electrode while a large gold substrate serves as our counter electrode.

Conductance histograms for TDO3-TDO5 in TCB

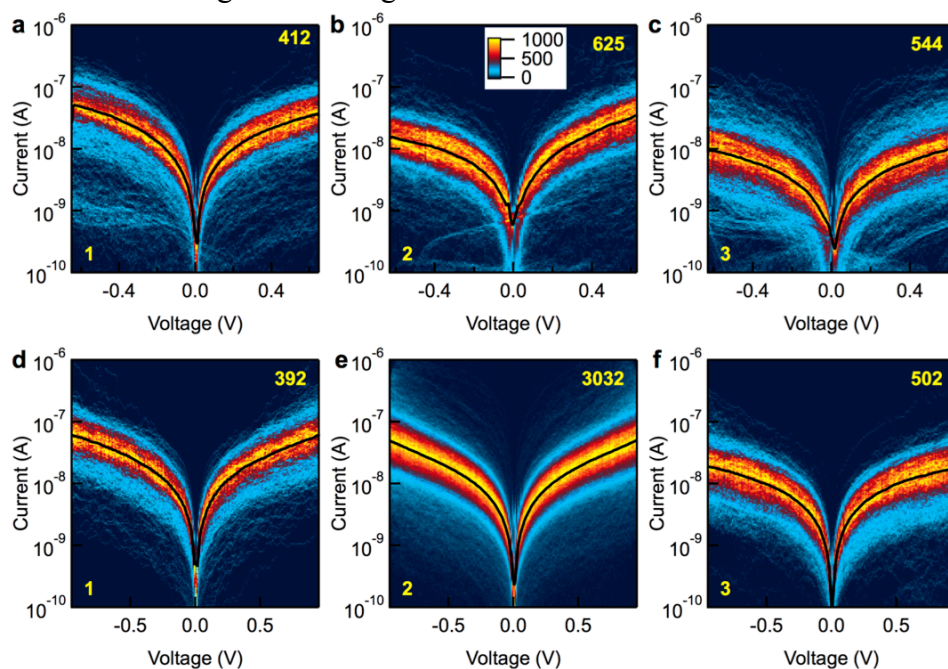


Supplementary Figure 6. Conductance histograms for TDO3-5 measured 1,2,4-trichlorobenzene (TCB). All histograms were measured prior to IV curves being collected.

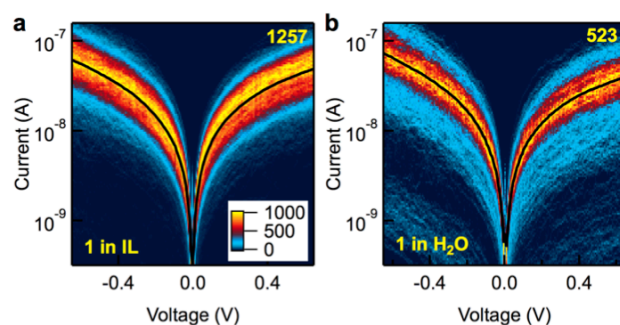
2D Current-Voltage (IV) histograms



Supplementary Figure 7. Two-dimensional IV histograms for TDO3-TDO5 in propylene carbonate (a-c) and 1,2,4-trichlorobenzene (d-f). Histograms were constructed from the number of traces indicated in the figures. Average IV curves are overlaid as solid black lines.



Supplementary Figure 8. Two-dimensional IV histograms for 4,4'-bipyridine (1), 4,4''-diamino-*p*-terphenyl (2), and 2,9-dithiadecane (3) in propylene carbonate (a-c) and 1,2,4-trichlorobenzene (d-f). Histograms were constructed from the number of traces indicated in the figures. Average IV curves are overlaid as solid black lines.



Supplementary Figure 9. Two-dimensional IV histograms for 4,4'-bipyridine (**1**) in additional polar media: (a) an ionic liquid (DEME-TFSI) and (b) H₂O. Histograms were constructed from the number of traces indicated in the figures. Average IV curves are overlaid as solid black lines.

II. Experimental Determination of Orbital Alignment

In order to determine the orbital alignment and orbital coupling strength in TDO4 single-molecule junctions, we make use of the following recently developed technique²:

- 1) Measure the conductance, G , and the derivative of conductance with respect to voltage (dG/dV) for a single molecule junction.
- 2) Obtain analytical expressions for these two quantities in terms of orbital energy and orbital coupling strength.
- 3) Iteratively solve a pair of non-linear equations to determine the two values.

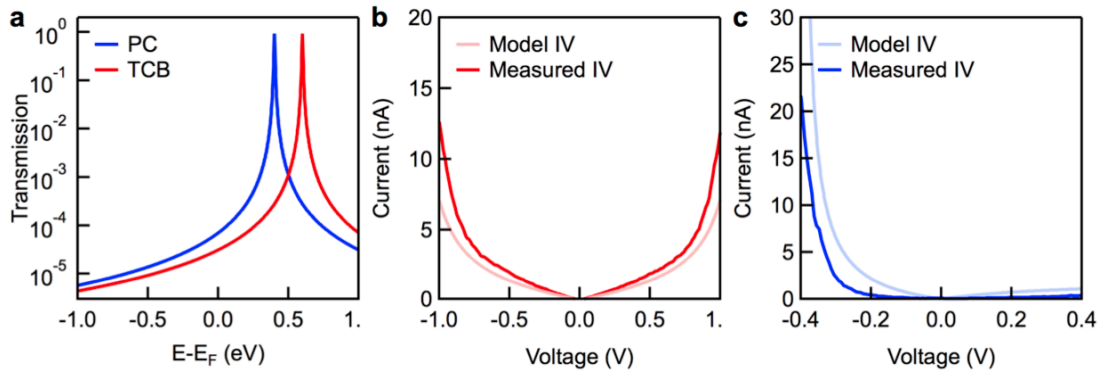
G and dG/dV are obtained by using a modified break-junction technique, similar to that of the IV measurements (see above). However, instead of applying a saw-tooth bias ramp while the tip is held at a fixed distance from the substrate, an additional AC voltage (65 mV at 16 kHz and 130 mV at 14 kHz in PC and TCB respectively) is applied on top of a DC voltage (-220 mV and 500 mV in PC and TCB respectively). As with IV measurements, we only analyze traces that have a molecule present in the junction while the hold is applied. We do this by checking that the conductance of the junction (just prior to the AC voltage being applied) falls within a standard deviation of the conductance histogram peak.

The frequency domain representation of the current while the AC voltage is applied is obtained using the discrete Fourier transform. The zero frequency signal corresponds to the DC current while the signal at the fundamental frequency (16 kHz and 14 kHz) corresponds to the AC current. The AC current consists of two components: the first is the tunneling current through the molecular junction and the second is the result of the capacitive coupling of the

electrodes. We only consider the current in phase with the applied AC voltage in order to discard the capacitive component. We also measure currents resulting from any non-linearity in the conductance-voltage relationship; these are measured at the second harmonic frequency (32 kHz and 28 kHz). In order to see explicitly what is responsible for this signal, the current through the junction is Taylor expanded around the DC value up to third order terms to yield:

$$I = \left[I(V_{DC}) + \frac{1}{4} \frac{dG}{dV} \bigg|_{V_{DC}} V_{AC}^2 \right] + \left[G|_{V_{DC}} + \frac{1}{8} \frac{d^2G}{dV^2} \bigg|_{V_{DC}} V_{AC}^2 \right] V_{AC} \sin(\omega_{AC} t) - \frac{1}{4} \frac{dG}{dV} \bigg|_{V_{DC}} V_{AC}^2 \cos(2\omega_{AC} t)$$

Here, I is the current through the junction, V_{DC} is DC bias voltage, V_{AC} is the amplitude of the AC voltage, and ω_{AC} is the frequency of AC voltage.

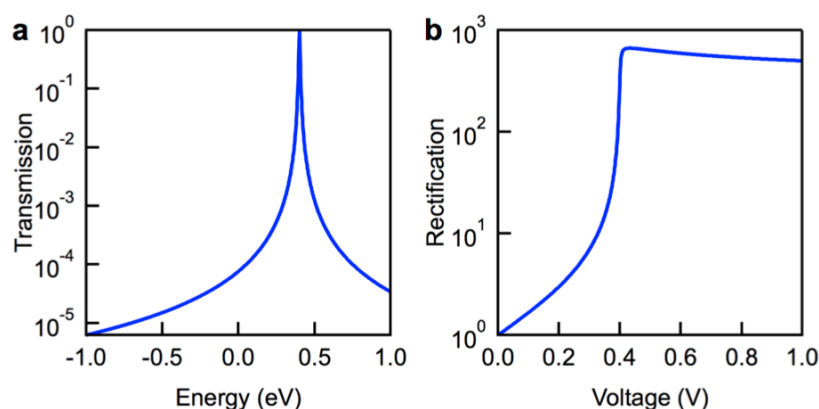


Supplementary Figure 10. (a) Model transmission functions created using the ϵ and Γ parameters extracted from AC measurements (see Figure 5). (b) Measured IVs for TDO4 in TCB compared with model IVs obtained by integrating the transmission function in (a) as detailed in the text. (c) The same analysis, using the model transmission function for PC. There is good agreement between the measured and calculated curves. Deviations between the model and measured IVs are primarily because IV measurements select a subset of junctions that sustain the entire bias ramp while the AC measurements are done at a fixed and smaller bias.

The terms in the first bracket represent the DC current due to the DC voltage and a rectification term ($(\frac{1}{4} \frac{dG}{dV} \big|_{V_{DC}} V_{AC}^2)$) due to a non-linearity in the conductance-voltage relationship. The second set of terms corresponds to the differential conductance (dI/dV) and a small contribution from second order conductance derivative with respect to voltage. The second harmonic term corresponds purely to the rectification term of the DC current. Thus, the second harmonic current measures dG/dV with small contributions from higher order terms. When the junction transmission function is well described by a single Lorentzian function (as given in

equation (2) of the manuscript), we can derive an analytic expression for the AC current that is in phase with the applied AC voltage at the fundamental frequency in terms of ε and Γ . Note that in this analysis, we explicitly include the dependence of the resonance position on the voltage through the α parameter as described in the main text. This gives one non-linear equation with two unknown parameters. Similarly, we derive a second analytic expression for the current at the second harmonic in terms of ε and Γ . Although not shown explicitly above, we include terms up to sixth order for the Taylor series expansion. We solve these two non-linear equations using a non-linear least squares solver algorithm to determine ε and Γ in a single molecule junction.

Rectification and Single-Lorentzian Model:



Supplementary Figure 11. Single Lorentzian model. (a) Single Lorentzian transmission function created using $\varepsilon = 0.4$ eV and $\Gamma = 7$ meV. (b) Rectification ratio ($I_{\text{on}}/I_{\text{off}}$, RR) as a function of applied voltage using the analytic expression from above. Within our model, we find RRs > 500 as the applied bias nears the value of the zero-bias molecular resonance in agreement with experiment.

In cases where transmission can be indeed modeled as a single Lorentzian function over a reasonably wide energy range, we are able to obtain an analytic expression for the rectification ratio at a given voltage. Assuming a transmission function of the form:

$$T(E) = \frac{\Gamma^2/4}{(E - \varepsilon - \alpha eV)^2 + \Gamma^2/4}$$

as defined in the main text. Assuming $\alpha=0.5$, we find:

$$RR = \frac{\int_{-eV/2}^{eV/2} T(E - \varepsilon + eV/2) dE}{\int_{-eV/2}^{eV/2} T(E - \varepsilon - eV/2) dE}$$

$$RR = \frac{\tan^{-1}\left(\frac{\varepsilon}{\Gamma/2}\right) - \tan^{-1}\left(\frac{\varepsilon - eV}{\Gamma/2}\right)}{\tan^{-1}\left(\frac{\varepsilon + eV}{\Gamma/2}\right) - \tan^{-1}\left(\frac{\varepsilon}{\Gamma/2}\right)}$$

Plotting this function (see Figure S11), we find, not surprisingly, that we would expect very large rectification ratios as the bias window nears the molecular resonance. Indeed, this simple picture predicts ratios on the order of what we have measured experimentally.

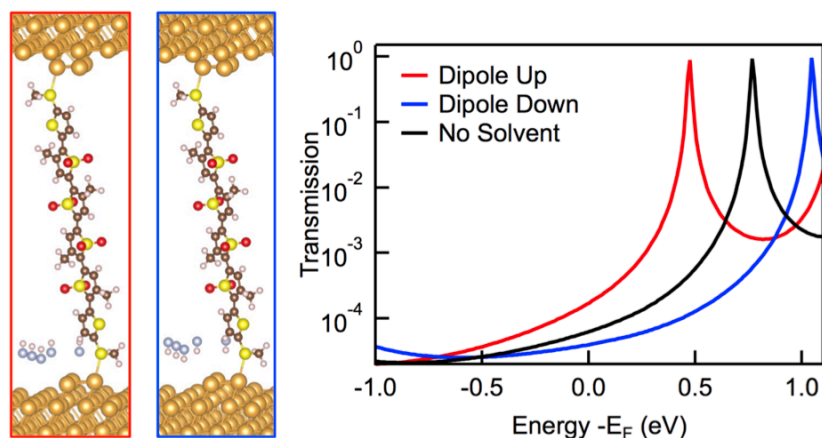
III. Computational Details for DFT+Sigma Method

The DFT+ Σ^3 method corrects the level alignments inherent to the Perdew-Burke-Ernzerhof (PBE) functional,⁴ by adding a self-energy correction⁵ to the converged PBE Kohn-Sham Hamiltonian and computing the transmission function with this modified Hamiltonian⁶. The self-energy correction is based on the GW method, and includes two parts: (1) gas-phase contribution, correcting inaccuracies in PBE eigenvalues for isolated molecule; and (2) surface polarization effect that is approximated by a classical image-charge model.⁵ For the TDO4 system, PBE places the LUMO, the dominant conducting orbital at 0.28 eV above E_F . The gas-phase correction shifts LUMO upwards by 1 eV and the surface polarization effect shifts LUMO downwards by 0.5 eV resulting in a net upward shift of 0.5 eV and placing the LUMO at about 0.78 eV above E_F . This LUMO position is in excellent agreement with the experimentally determined position in 1,2,4-trichlorobenzene as shown in Figure 5b.

To model the effect of PC molecules on level alignment in TDO4 molecular junction, we add three PC molecules on both gold surfaces in a unit cell oriented with the oxygen on the Au (111) surface. The distance between the oxygen atom of PC and the top Au (111) surface is about 2.5 Å and the binding energy between the PC molecule and the Au (111) surface is about 0.2 eV. When compared to junctions without PC, we find the LUMO peak in $T(E)$ is shifted downwards by about 0.3 eV, again in excellent agreement with the experimentally determined shift of 0.2 eV (Figure 5b).

To model the effects of a dense electric layer on one electrode, we have computed zero bias transmission functions with the addition of 5 hydrofluoric acid (HF) molecules to one electrode, with the HF dipole being oriented either up or down (Figure S12). The HF molecules are added to the relaxed TDO4 junction; no further structural relaxation is done after the HF is added. The HF bond (and therefore the dipole moment) is kept perpendicular to the Au surface.

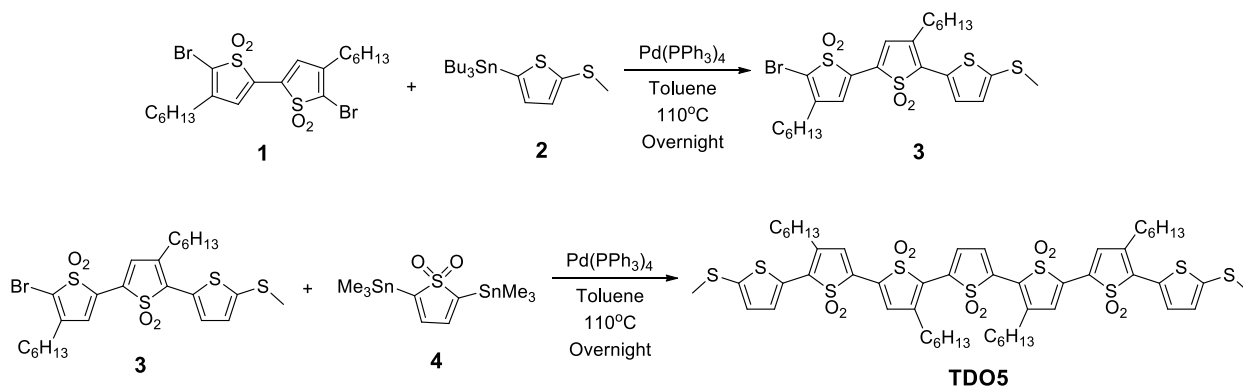
The lower atom in the HF molecule is kept 5 Å above the surface to ensure that the molecule is not bound.



Supplementary Figure 12. Junction structures and junction transmission functions for TDO4, using hydrofluoric acid (HF) as a dipole to simulate the effects of a dense electric double layer on one electrode; the dipole orientation is used as a proxy to simulate the effects of an applied bias. Zero bias transmission functions are calculated without solvent (black), with the HF dipole oriented “up” (red) and with the HF dipole oriented “down” (blue). It can be clearly seen that the effect of the dipole is to shift the molecular resonance relative to E_F .

IV. TDO5: Synthesis & Characterization

Commercially available starting materials were purchased from Sigma-Aldrich and used as received, unless otherwise noted. All reactions were performed in oven-dried round bottom flasks using standard schlenk techniques, unless otherwise noted. ^1H and ^{13}C nuclear magnetic resonance spectra were recorded at 300 K (unless otherwise noted) on Bruker DRX300 (300MHz) or Bruker DRX400 (400MHz) FT-NMR spectrometers. High-resolution mass spectra were recorded on a JMS-HX110 HF mass spectrometer (ionization mode: FAB+). Uv-vis absorption spectra were taken on a Shimadzu UV-1800 spectrophotometer. Compounds **1** and **2** were synthesized by previously published procedures.^{7,8}

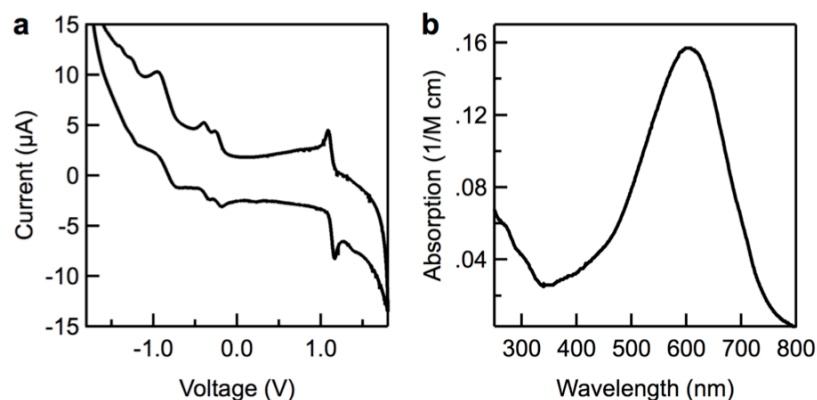


Synthesis of compound **3**: Compound **1** (1.67 g 3 mmol) and compound **2** (1.26 g, 3 mmol) were dissolved in 30 mL toluene, under nitrogen. Pd(PPh₃)₄ (173 mg, 0.15 mmol) was added and the resulting mixture was stirred at 80 °C for 2 h. After cooling to room temperature, the reaction mixture was extracted with CH₂Cl₂, washed twice with water, and then dried with Na₂SO₄. After removing the solvent, the crude product was purified by column chromatography on silica gel, and eluted with 25% EtOAc/hexanes to yield compound **3** as red solid (0.82 g, yield: 46%).

Synthesis of compound **4**: 2,5-bis(trimethylstannyl)thiophene (1.74 g, 4.25 mmol) was dissolved in 60 mL CH₂Cl₂, and the mixture was cooled to 0 °C. 2.2 equivalents of Rozen's reagent⁹ (HOF·CH₃CN, 60 mL, 0.14 M) was then added to the reaction flask. The reaction was stopped after 30 min and the excess HOF·CH₃CN was quenched with saturated sodium bicarbonate. The mixture was poured into water and extracted with CH₂Cl₂; the organic was layer dried over sodium sulfate. After removing the solvent, the crude product was purified by recrystallization in ethanol to give compound **4** as a white solid 0.48 g, yield: 26%. ¹H NMR (400 MHz, CDCl₃, ppm): δ 0.43 (s, 18 H), 6.69 (s, 2H).

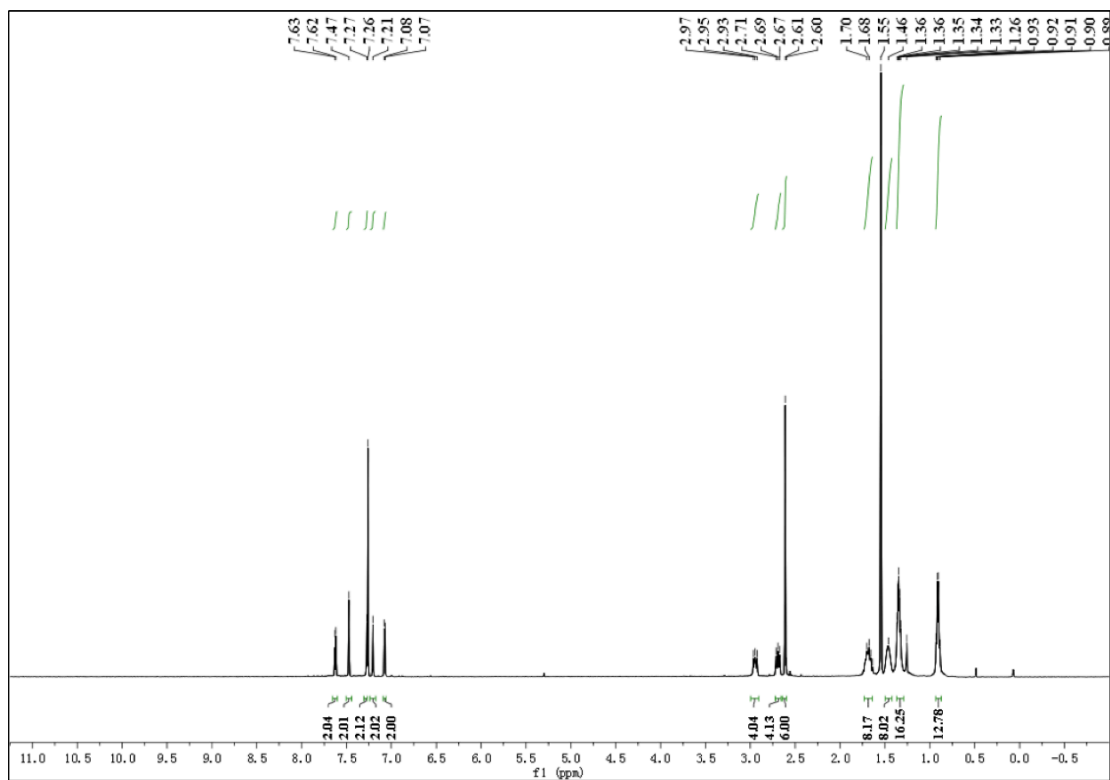
Synthesis of **TDO5**: Compound **4** (26 mg, 0.058 mmol), compound **3** (70 mg, 0.116 mmol), and Pd(PPh₃)₄ (4 mg, 0.003 mmol) were charged in a 20-mL reaction vial, the reaction vial was purged with nitrogen and securely sealed. The reaction mixture was stirred at 110 °C for 18 h before it was cooled to room temperature. After removal of the solvent, the dark crude product was purified by chromatography on silica gel using 60% dichloromethane in hexanes as eluent, the titled compound was obtained as a dark solid (53 mg, 78%). ¹H NMR (400 MHz, CDCl₃, ppm): δ 0.88-0.93 (m, 12H), 1.33-1.36 (m, 16H), 1.46 (m, 8H), 1.63-1.70 (m, 8H), 2.61 (s, 6H), 2.69 (t, *J* = 8 Hz, 4H), 2.94 (t, *J* = 8 Hz, 4H), 7.07 (d, *J* = 4 Hz, 2H), 7.20 (s, 2H), 7.27 (s, 2H),

7.47 (s, 2H), 7.62 (d, $J = 4$ Hz, 2H). ^{13}C NMR (100 MHz, CDCl_3 , ppm): δ 13.97, 20.45, 22.45, 22.47, 27.30, 28.82, 29.23, 29.69, 30.36, 31.36, 31.42, 31.98, 125.90, 126.51, 127.26, 127.46, 128.77, 129.09, 130.62, 130.93, 131.56, 133.36, 133.88, 144.87, 145.51. HRMS (FAB) m/z calcd for $\text{C}_{54}\text{H}_{68}\text{O}_{10}\text{S}_9$: 1165.70. Found $(\text{M}+\text{Na})^+$: 1186.68.

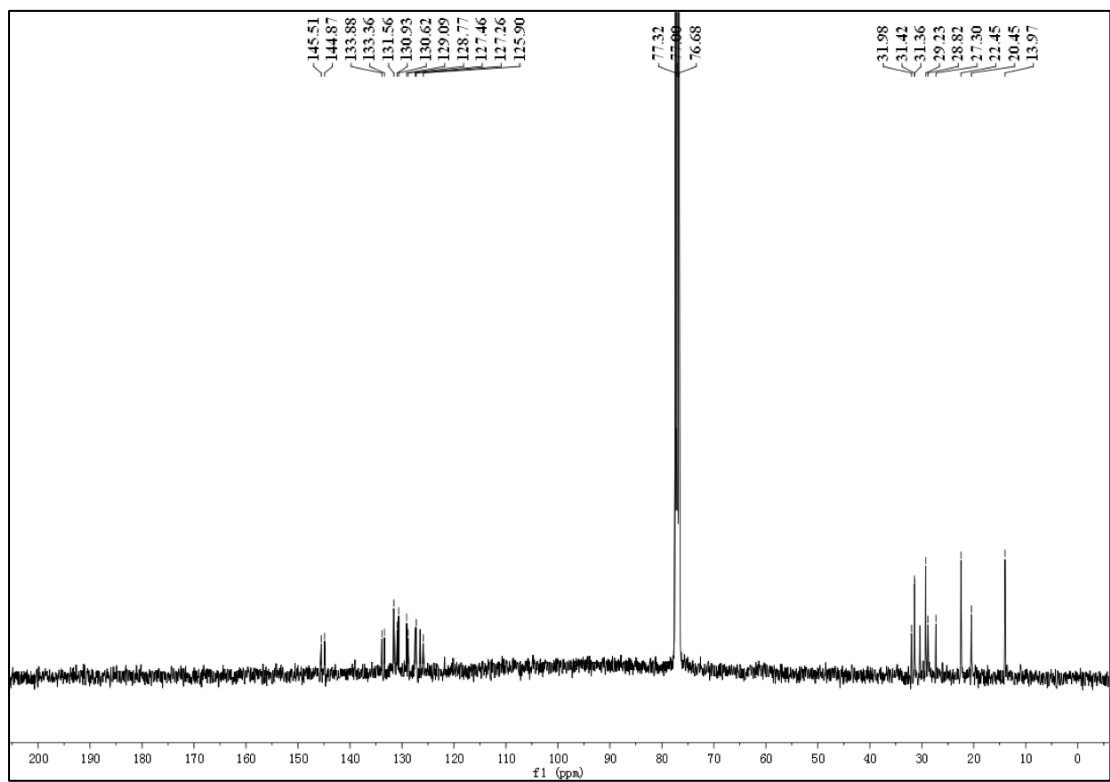


Supplementary Figure 13. (a) Cyclic voltammogram of TDO5 performed using a 10mM solution of TDO5 with 100mM tetrabutylammonium hexafluorophosphate ($t\text{-Bu}_4\text{NPF}_6$) as supporting electrolyte in dichloromethane. The measurement was made using a standard three-electrode set up, with Pt disk, Pt wire, and Ag/AgCl electrodes serving as the working electrode, counter electrode, and reference electrode, respectively. For calibration, the redox potential of ferrocene/ferrocenium (Fc/Fc^+) was measured under the same conditions, and is located at 0.31V relative to the Ag/AgCl electrode. (b) UV-vis spectrum of TDO5 performed using a 10 μM solution of TDO5 in dichloromethane.

NMR Spectra for TDO5:



¹H NMR of TDO5



¹³C NMR of TDO5

V. References

- 1 Quek, S.Y., Choi, H.J., Louie, S.G., & Neaton, J.B., Length Dependence of Conductance in Aromatic Single-Molecule Junctions. *Nano Lett.* 9 (11), 3949-3953 (2009).
- 2 Adak, O., Korytar, R., Joe, A.Y., Evers, F., & Venkataraman, L., Impact of Electrode Density of States on Transport through Pyridine-Linked Single Molecule Junctions. *arXiv:1504.00242* (2015).
- 3 Quek, S.Y. *et al.*, Amine-gold linked single-molecule circuits: Experiment and theory. *Nano Lett.* 7 (11), 3477-3482 (2007).
- 4 Perdew, J.P., Burke, K., & Ernzerhof, M., Generalized Gradient Approximation Made Simple. *Phys. Rev. Lett.* 77 (18), 3865-3868 (1996).
- 5 Neaton, J.B., Hybertsen, M.S., & Louie, S.G., Renormalization of molecular electronic levels at metal-molecule interfaces. *Phys. Rev. Lett.* 97 (21), 216405 (2006).
- 6 Liu, Z.-F. *et al.*, Control of Single-Molecule Junction Conductance of Porphyrins via a Transition-Metal Center. *Nano Lett.* 14 (9), 5365-5370 (2014).
- 7 Amir, E. *et al.*, Synthesis and characterization of soluble low-bandgap oligothiophene-[all]-S,S-dioxides-based conjugated oligomers and polymers. *Journal of Polymer Science Part A: Polymer Chemistry* 49 (9), 1933-1941 (2011).
- 8 Barbarella, G. *et al.*, Bright Oligothiophene N-Succinimidyl Esters for Efficient Fluorescent Labeling of Proteins and Oligonucleotides. *Bioconjugate Chemistry* 17 (1), 58-67 (2005).
- 9 Amir, E. & Rozen, S., Synthesis of [all]-S,S-dioxide oligothiophenes using HOF center dot CH₃CN. *Angew. Chem. Int. Ed.* 44 (45), 7374-7378 (2005).